

Tensile Plasticity in Metallic Glasses with Pronounced β Relaxations

H. B. Yu, X. Shen, Z. Wang, L. Gu, W. H. Wang, and H. Y. Bai*

Institute of Physics, Chinese Academy of Sciences, Beijing 100190, China

(Received 29 June 2011; published 4 January 2012)

Metallic glasses are commonly brittle, as they generally fail catastrophically under uniaxial tension. Here we show pronounced macroscopic tensile plasticity achieved in a La-based metallic glass which possesses strong β relaxations and nanoscale heterogeneous structures. We demonstrate that the β relaxation is closely correlated with the activation of the structural units of plastic deformations and global plasticity, and the transition from brittle to ductile in tension and the activation of the β relaxations follow a similar time-temperature scaling relationship. The results have implications for understanding the mechanisms of plastic deformation and structural origin of β relaxations as well as for solving the brittleness in metallic glasses.

DOI: 10.1103/PhysRevLett.108.015504

PACS numbers: 62.20.F-, 61.43.Dq, 81.05.Kf

Metallic glasses (MGs) have excellent physical, chemical, and mechanical properties, but their practical applications have been impeded due to their brittleness [1–4]. Although some MGs show considerable plastic strain under constrained deformations such as compression and bending [5], the unconstrained tensile plasticity of MGs is almost zero [1]. Substantial effort has been made to enhance the tensile ductility of MGs [6–11], and most of the approaches used generally involve microstructure optimizations, such as crystalline dendrite reinforced MG composites [6], and deformation-induced martensites and nanotwins [7,8]. So far, significant tensile ductility of monolithic MGs has been achieved only at nanoscales [9–11]. Therefore, it is a challenge to obtain MGs with macroscopic tensile ductility at room temperature. Meanwhile, the lack of tensile plasticity also hinders studies on some fundamental issues, such as the mechanisms of plastic deformations [12].

The underlying relaxations of glass-forming liquids and glasses are governed by two main processes: the primary relaxation (α relaxation) and the secondary relaxation (β relaxation) [13]. The α relaxation involves large scale rearrangements of materials and is responsible for the glass transitions [14]. As the α relaxation is frozen below glass transition temperature T_g , the localized and reversible β relaxation is the principal source of the dynamics in a glassy state [15]. In metallic glasses, it was recently found that the β relaxations have the same values of activation energy as those of the basic structural units of plastic deformation [shear transformation zones (STZs)] [16–20]. The local cooperative motions of atoms responsible for β relaxations act as “potential STZs” that accommodate the plastic deformation, and both STZs and β relaxations are related to the heterogeneous atomic structures of MGs [18]. It is then expected that MGs with pronounced β relaxations would have abundant potential STZs, which will self-organize into plentiful shear bands and accommodate the plastic deformation. Therefore, such

MGs might be macroscopically ductile. However, for the known MGs, their β relaxations are rather obscure [18]. They are manifest as either broad humps or excess wings and are closely merged into the α relaxations, and this makes a critical scrutiny of the correlations between the β relaxations and mechanical properties difficult.

In this work, we report a $\text{La}_{68.5}\text{Ni}_{16}\text{Al}_{14}\text{Co}_{1.5}$ MG which shows unusually strong β relaxations and macroscopic tensile plasticity. We show that the transition from brittle to ductile in tension and the activation of β relaxations follow a similar time-temperature scaling relationship, and the activations of β relaxations endow the MG with remarkable deformability. The structural origin for the pronounced tensile deformability and the distinct β relaxations of the MG were also studied.

Metallic glass ribbons with a nominal composition of $\text{La}_{68.5}\text{Ni}_{16}\text{Al}_{14}\text{Co}_{1.5}$ (T_g is 445 K) were prepared by melt spinning (See Materials and Methods in Supplemental Material [21] for details). Their glassy nature was ascertained by x-ray diffraction (MAC Mo3 XHF diffractometer with Cu $K\alpha$ radiation, Fig. S1 [21]), a differential scanning calorimeter (PerkinElmer DSC-7, Fig. S2 [21]), and transmission electron microscopy (TEM) (Tecnai F20). The dynamical mechanical behaviors of the MGs were tested on a TA Q800 dynamical mechanical analyzer. Uniaxial tensile tests of metallic glass ribbons were carried out over a temperature range (253–373 K) and strain rate range (1.6×10^{-6} to 10^{-3} s $^{-1}$) in the same dynamical mechanical analyzer machine.

The mechanical properties of the MG are tested in quasi-static tensions, and Fig. 1 shows the representative stress-strain curves for the MG at different strain rates and temperatures. In Fig. 1(a), at and below 273 K, the MG fails in a brittle manner. While at room temperature (RT, ~ 300 K), clear yielding and notable tensile plastic strain ($\sim 0.7\%$) can be observed, and the tensile plasticity increases remarkably with temperature increases. This might be the first macroscopic MG sample with tensile plasticity at or near

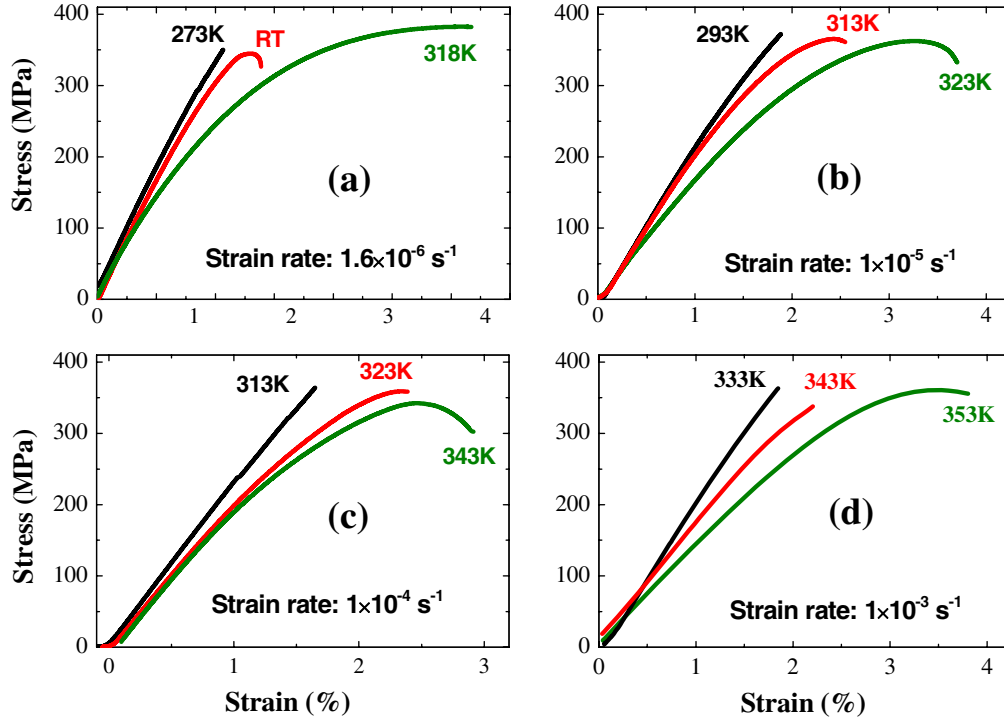


FIG. 1 (color online). The engineering stress-strain curves (in tension) tested at strain rates (a) 1.6×10^{-6} , (b) 1×10^{-5} , (c) 1×10^{-4} , and (d) $1 \times 10^{-3} \text{ s}^{-1}$. For clarity, only three representative stress-strain curves corresponding to three different testing temperatures are shown in each figure.

RT, and the existing reported tensile plasticity of MGs at RT is limited only to composite materials [6–8] or under extremely high strain rates [22,23] or at nanoscales [9–11].

The mechanical properties of the MG are strain-rate-dependent. For instance, tensile plastic strain begins to appear at about 313 K under $1 \times 10^{-5} \text{ s}^{-1}$ [Fig. 1(b)], while it is at about 323 K under $1 \times 10^{-4} \text{ s}^{-1}$ [Fig. 1(c)] and further increases to 343 K when tested at $1 \times 10^{-3} \text{ s}^{-1}$ [Fig. 1(d)] (see Fig. S3 for additional characterizations [21]). Figure 2(a) summarizes the tension test data in a deformation mode map over the range from 273 to 363 K and strain rates between 1×10^{-5} and $1 \times 10^{-3} \text{ s}^{-1}$. To compare with the established deformation map of MGs [2], the testing temperature is scaled by T_g . Two distinct regimes of deformation modes can be observed for the La-based MG: the brittle regime at low temperatures or high strain rates and the ductile regime at relatively high temperatures (from $0.67T_g$ to $0.9T_g$) and low strain rates. Interestingly, both of the regimes are not in the homogeneous flow regime associated with the supercooled liquid (or α relaxations) as shown in Fig. 2(a). The results suggest that the La-based MGs have tensile ductility in its glassy states, in sharp contrast to many other known MGs, for which brittleness is maintained very close to T_g , even in constrained deformations (see Fig. S4 for comparison). For example, the Cu-, Zr-, and Ti-based MGs show exclusively brittle behavior from $0.7T_g$ to $0.9T_g$, and the

Ce-based MGs with similar T_g to the La-MzG are purely brittle even under the test temperature of $0.92T_g$ and the strain rate of 10^{-4} s^{-1} [24]. Figure 2(a) also reveals a distinct boundary between the two regimes which describes the ductile to brittle transition (DBT) in the MG [25]. Figure 2(b) plots the strain-rate-dependent temperature of the DBT and fitted with an Arrhenius relation $\dot{\epsilon} = \dot{\epsilon}_0 \exp(-\Delta E_{\text{DBT}}/RT)$ [26]. The Arrhenius relation captures the DBT reasonably well and gives the apparent DBT activation energy $\Delta E_{\text{DBT}} \approx 103 \pm 10 \text{ kJ/mol}$ and the prefactor $\dot{\epsilon}_0 \approx 8 \times 10^{16} \text{ s}^{-1}$. In the ductile regime of Fig. 2(a), the MG can undertake intensive tensile deformations such as being elongated up to engineering strain 30% as shown in Fig. 2(c) (at 353 K or $0.79T_g$, and 90 K below T_g , and $1 \times 10^{-5} \text{ s}^{-1}$). Such a large elongation can be obtained only in supercooled liquid states in conventional MGs. Figure 2(d) shows a typical scanning electron microscope image of the fracture surface of the MG with a total strain of about 6% ($0.75T_g$ and $1 \times 10^{-5} \text{ s}^{-1}$), in which plenty of wavy shear bands are identified, suggesting that the tensile plastic deformation or fracture is highly inhomogeneous (see Fig. S5 for more evidence) and not the homogeneous viscous flow near T_g associated with the activation of α relaxations or supercooled liquid.

To understand the distinct tensile ductility and its relation with the relaxations of the MG, we characterized the

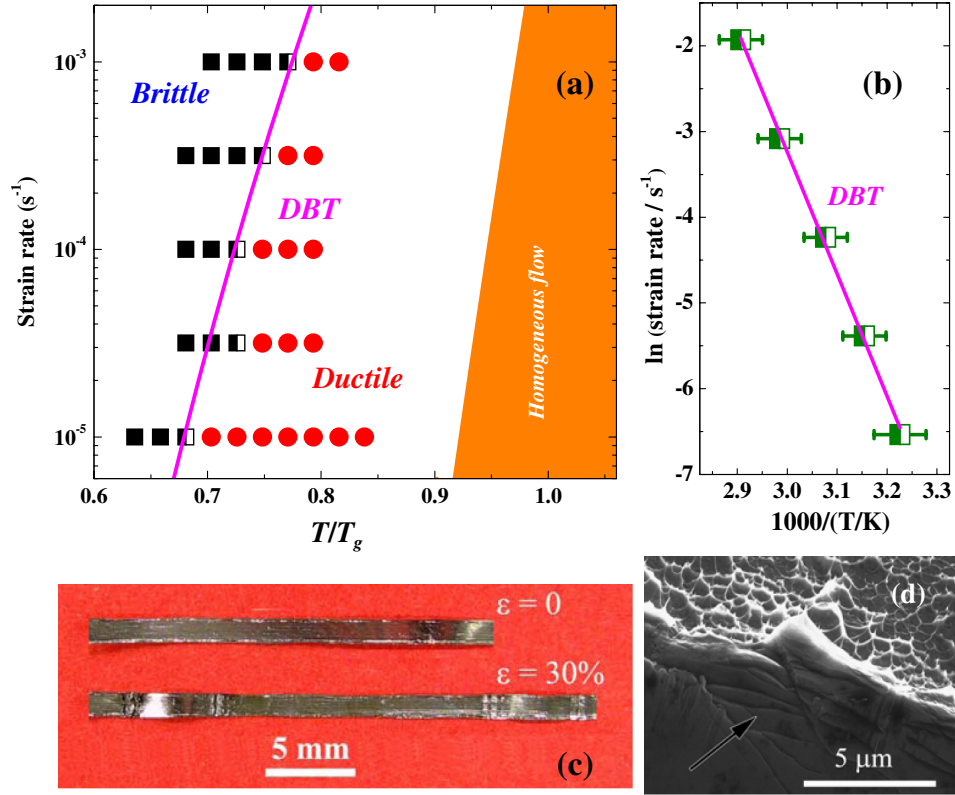


FIG. 2 (color online). (a) The deformation mode map summarizing the tension tests at different temperature and strain rates; the filled squares denote the brittle fracture while filled circles are for the ductile fracture, and the DBT is represented by half-filled squares. (b) The temperature and strain rate dependence of the temperature of DBT and fitted with the Arrhenius relation. (c) The photograph of the La-MG before and after tension with strain 30% (at 353 K and $1 \times 10^{-5} \text{ s}^{-1}$). (d) The scanning electron microscope image of a ductile fracture surface of the La-MG (at 333 K and $1 \times 10^{-5} \text{ s}^{-1}$ and total strain 6%), and the arrow indicates the shear bands.

relaxation behaviors of the MG with dynamical mechanical spectroscopy, which is a sensitive tool for detecting atomic rearrangements associated with defects in solids [15]. Figure 3(a) shows the temperature-dependent loss modulus E'' of the MG. On the increasing backgrounds of E'' curves, a relaxation peak can be observed around $0.6T_g - 0.8T_g$ (250–400 K) for the MG. The presence of E'' peaks indicates that the periodic testing strain is resonant with the local atomic motions associated with the β relaxations (see Fig. S6 for more dynamical mechanical spectroscopy characterizations [21]). Figure 3(a) also compares the β relaxation behaviors between our La-based MG with other ten typical MGs (those with different values of T_g and covering most of the common MG compositions). The β relaxations in other MGs exhibit as either broad humps (Pd- and conventional La-based MGs) or excess wings (Cu-, Zr-, and Ce-based MGs) and are almost merged into α relaxations. Clear and complete β relaxation peaks can be observed only in our La-based MG. The pronounced β relaxation peaks imply that certain types of intrinsic motions can be activated in the glassy state, which might be beneficial for the plastic deformations.

Figure 3(b) shows temperature-dependent E'' of the MG with discrete testing frequencies (f) ranging from 0.5 to 16 Hz. The inset in Fig. 3(b) shows the f dependence of the peak temperature and end-set temperature (which is the minimum in loss between the β and α relaxation peaks) of β relaxations and fitted with Arrhenius relations, $f = f_\infty \exp(-E_\beta/RT)$, where f_∞ is the prefactor and E_β is the activation energy of the β relaxation. The E_β is determined to be $91 \pm 4 \text{ kJ/mol}$ from the peak shift and $98 \pm 8 \text{ kJ/mol}$ from the end-set shift, respectively. The value $E_\beta/RT_g \approx 25 \pm 3$ is consistent with the empirical relationship $E_\beta/RT_g \approx 26$ found in various MGs and non-metallic glasses [18,27]. We emphasize that the value of E_β is nearly equivalent to the apparent activation energies of DBT ($\Delta E_{\text{DBT}} \approx 103 \pm 10 \text{ kJ/mol}$) and the STZ event [18]. In a wide range of crystalline materials, the apparent activation energy ΔE_{DBT} of DBT is equal to the activation energy for dislocation glide (known as the Peierls stress), clearly revealing the underlying deformation mechanisms [26]. From the similar values of activation energy, we infer that the DBT of the MG is closely related to the events of STZs and the β relaxations.

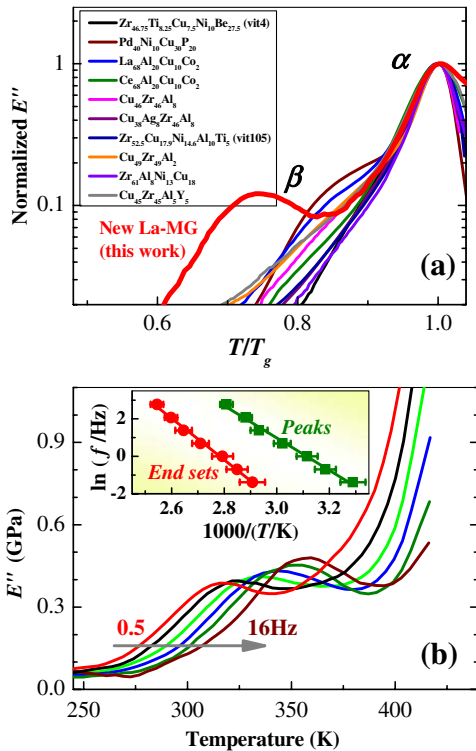


FIG. 3 (color online). (a) Comparison of the behavior of β relaxations between the La-based MG with ten other typical MGs. For comparison, the temperature is scaled by T_g and the loss modulus E'' (1 Hz) is normalized by a corresponding maximum (at T_g). (b) Temperature-dependent E'' of the La-MG showing distinct β relaxations peaks; the frequencies used are 0.5, 1, 2, 4, 8, and 16 Hz from left to right, respectively. The inset shows the frequency dependence of the peak and end-set temperature of the β relaxations and fitted with Arrhenius relations.

In polymer glasses, there is an empirical relation between strain rates $\dot{\epsilon}$ and f [28], $f = A\dot{\epsilon}$, with constant $A \approx 143$. Using this relation, we translated the strain rates in tensile tests into the effective frequencies and then obtained a direct relationship between the β relaxations and the DBT of the MG. As shown in Fig. 4, the Arrhenius plots of end sets of the β relaxations and DBT collapse into a single master line within errors, and they almost coincide with each other when extrapolated. The results indicate that the activation of β relaxations is an indicator for achieving tensile plasticity of the MG, and the mechanical properties can be understood from the perspective of β relaxations.

To correlate the distinct behaviors of β relaxations and the deformability of the MG with its structure, TEM investigations were performed to reveal microstructural features of the MG. Figure 5(a) shows a scanning TEM image of the as-cast La-based MG, where the contrast is directly related to the atomic number (Z -contrast image). The most notable structural characteristic is that the MG is composed

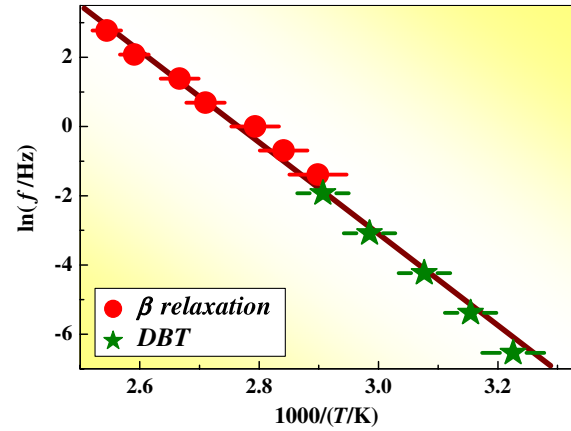


FIG. 4 (color online). The Arrhenius plot of temperature and effective frequencies dependent on DBT and the end set of the β relaxation of the La-based MG.

of two types of collagelike regions: Light regions with typical sizes ranging from 50 to 200 nm are enveloped by dark boundary regions, which are about 5–20 nm in width. These regions are tightly packed and can also be observed from bright-field TEM micrographs (see Fig. S7 [21]). High-resolution TEM [Fig. 5(b)] and the selected-area electron diffractions [the inset in Fig. 5(b)] further confirm that both of the two regions are of a glassy nature, excluding the possible nanocrystallizations. Energy-dispersive x-ray spectroscopy and compositional profiling experiments reveal that the dark regions contain more Ni but less La elements than the light regions, whereas the distributions of Al atoms are relatively homogeneous (Fig. S8 [21]). The inhomogeneous distributions of La and Ni atoms, which could be induced by decomposition, result in the heterogeneous structures and play a crucial role in the mechanical behavior [5] and β relaxations of MGs [29–31]. It is proposed [29–31] that the local atomic motions in soft regions are responsible for the β relaxations, and the heterogeneous structure improves the plasticity of MGs through the formation of multiple shear bands [5].

Our observations reveal the structural features of the MG with pronounced β relaxations and corroborate the proposition that β relaxations are correlated with structural heterogeneity and mechanical properties [18,29]. A plausible picture regarding the structural heterogeneity, β relaxations, and tensile plasticity could then be suggested. The heterogeneous structure might be related to the unusual β relaxations of the MG, and the β relaxations and STZ events then follow a similar activation mechanism. The pronounced β relaxations of the MG indicate that the MG has abundant potential STZs, and global tensile plasticity can then be triggered when the high density potential STZs are activated to reach the percolation limit by external stresses [17]. Consequently, the transition from brittle to ductile in tension is a direct indication of the activation

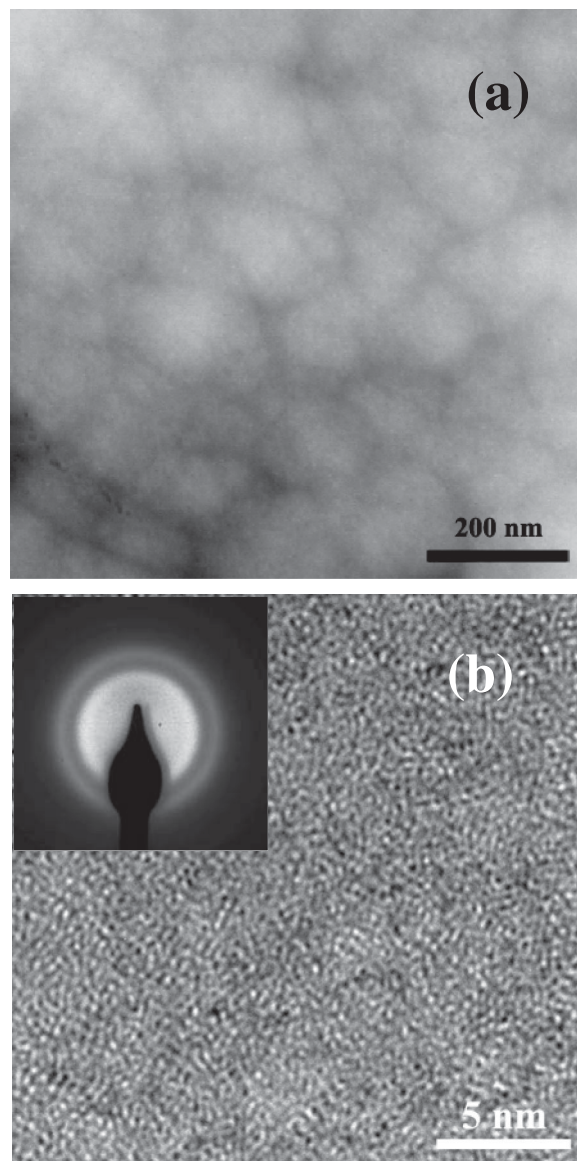


FIG. 5. (a) A scanning TEM image of the as-cast La-MG. (b) A high-resolution TEM micrograph of the as-cast La-MG; the inset shows the selected-area electron diffraction.

of the high density potential STZs or the β relaxations driven by applied stress.

We also find that the relaxation behaviors of MGs are sensitive to their compositions. Minor additions of Cu (about 5%) to present La-based MG completely change the β relaxation behavior (Fig. S9 [21]). This result indicates that pronounced β relaxations might also be obtained in other MG systems. The β relaxations behavior could be used as an indicator for solving the problem of brittleness of metallic glasses. We anticipate that the tensile ductility could be realized in other MGs through enhancement of the β relaxations in MGs.

This work was supported by MOST 973 (No. 2010CB731600) and the NSF of China (No. 50731008 and No. 50921091).

*To whom all correspondence should be addressed.
hybai@aphy.iphy.ac.cn

- [1] A. L. Greer, *Mater. Today* **12**, 14 (2009).
- [2] C. A. Schuh, T. C. Hufnagel, and U. Ramamurty, *Acta Mater.* **55**, 4067 (2007).
- [3] W. H. Wang, *Adv. Mater.* **21**, 4524 (2009).
- [4] J. Schroers *et al.*, *Mater. Today* **14**, 14 (2011).
- [5] Y. H. Liu *et al.*, *Science* **315**, 1385 (2007).
- [6] D. C. Hofmann *et al.*, *Nature (London)* **451**, 1085 (2008).
- [7] S. Pauly, S. Gorantla, G. Wang, U. Kuhn, and J. Eckert, *Nature Mater.* **9**, 473 (2010).
- [8] Y. Wu, Y. Xiao, G. Chen, C. T. Liu, and Z. Lu, *Adv. Mater.* **22**, 2770 (2010).
- [9] J. H. Luo, F. F. Wu, J. Y. Huang, J. Q. Wang, and S. X. Mao, *Phys. Rev. Lett.* **104**, 215503 (2010).
- [10] D. C. Jang and J. R. Greer, *Nature Mater.* **9**, 215 (2010).
- [11] H. Guo *et al.*, *Nature Mater.* **6**, 735 (2007).
- [12] M. L. Falk, *Science* **318**, 1880 (2007).
- [13] P. G. Debenedetti and F. H. Stillinger, *Nature (London)* **410**, 259 (2001).
- [14] C. A. Angell, K. L. Ngai, G. B. McKenna, P. F. McMillan, and S. W. Martin, *J. Appl. Phys.* **88**, 3113 (2000).
- [15] K. L. Ngai and M. Paluch, *J. Chem. Phys.* **120**, 857 (2004).
- [16] W. L. Johnson and K. Samwer, *Phys. Rev. Lett.* **95**, 195501 (2005).
- [17] J. S. Harmon, M. D. Demetriou, W. L. Johnson, and K. Samwer, *Phys. Rev. Lett.* **99**, 135502 (2007).
- [18] H. B. Yu, W. H. Wang, H. Y. Bai, Y. Wu, and M. W. Chen, *Phys. Rev. B* **81**, 220201 (2010).
- [19] P. Schall, D. A. Weitz, and F. Spaepen, *Science* **318**, 1895 (2007).
- [20] M. L. Falk and J. S. Langer, *Phys. Rev. E* **57**, 7192 (1998).
- [21] See Supplemental Material at <http://link.aps.org/supplemental/10.1103/PhysRevLett.108.015504> for experimental details and Figs. S1–S9.
- [22] A. V. Sergueeva, N. A. Mara, D. J. Branagan, and A. K. Mukherjee, *Scr. Mater.* **50**, 1303 (2004).
- [23] Y. Yokoyama, K. Fujita, A. R. Yavari, and A. Inoue, *Philos. Mag. Lett.* **89**, 322 (2009).
- [24] B. Zhang, D. Q. Zhao, M. X. Pan, W. H. Wang, and A. L. Greer, *Phys. Rev. Lett.* **94**, 205502 (2005).
- [25] C. B. Picallo, J. M. López, S. Zapperi, and M. J. Alava, *Phys. Rev. Lett.* **105**, 155502 (2010).
- [26] M. Tanaka, E. Tarleton, and S. G. Roberts, *Acta Mater.* **56**, 5123 (2008).
- [27] K. L. Ngai, *Phys. Rev. E* **57**, 7346 (1998).
- [28] C. D. Xiao, J. Y. Jho, and A. F. Yee, *Macromolecules* **27**, 2761 (1994).
- [29] T. Ichitsubo *et al.*, *Phys. Rev. Lett.* **95**, 245501 (2005).
- [30] Y. H. Liu *et al.*, *Phys. Rev. Lett.* **106**, 125504 (2011).
- [31] H. Wagner *et al.*, *Nature Mater.* **10**, 439 (2011).